Bull. Chem. Soc. Jpn., **68**, 566—573(1995)

Observation of Nuclear Excitation by Electron Transition (NEET) in ^{197}Au with a Nanosecond Stroboscopic Electron Spectrometer

Atsushi Shinohara,[*, #] **Tadashi Saito, Kiyoteru Otozai,** [##] **Hiromu Fujioka,**[†, ###] **and Katsumi Ura**[†, ####]

Department of Chemistry and Laboratory of Nuclear Studies, Faculty of Science, Osaka University, Toyonaka, Osaka 560

†Department of Electronic Engineering, Faculty of Engineering, Osaka University, Yamada-Oka, Suita, Osaka 565

(Received July 4, 1994)

Nuclear excitation by electron transition (NEET) was investigated on ^{197}Au. It is expected for ^{197}Au that the deexcitation of the K-shell ionized atoms would be accompanied by the nuclear excitation of the first excited level. Time spectra of 63-keV electrons emerging from a ^{197}Au target after bombardment with 100-keV pulsed electron beam were measured with a specially designed nanosecond stroboscopic electron spectrometer. A decay component with a half-life of 1.9 ns was extracted from the electron time spectrum. The decay was attributed to the internal conversion electrons emitted from the excited ^{197}Au nucleus as a consequence of the NEET process and the NEET probability was deduced to be $P=(5.1\pm3.6)\times10^{-5}$. The result was compared with several theoretical estimates.

Nuclear excitation often takes place in the cascade transition of an orbital muon in muonic atoms, resulting in perturbed X-ray emission, neutron emission, or prompt fission.[1—7] The excitation effect has also been observed in pionic atoms.[8] In ordinary electronic atoms, the probability of exciting the nucleus by radiationless electronic transition is usually negligibly small compared to the X-ray or Auger-electron emission because the electronic transition energy is always low compared to the nuclear one and the interaction energy between the nucleus and its orbital electrons is very small. The excitation effect, however, may be observed in special cases where an atomic deexcitation energy closely matches a nuclear excitation energy and both transitions have a common multipolarity.[9] This phenomenon, called nuclear excitation by electron transition (NEET), has been observed in ^{189}Os[10—13] and ^{237}Np.[14] NEET proceeds through the electric quadrupole (E2) interaction in ^{189}Os, and through the electric dipole (E1) interaction in ^{237}Np.

Such phenomena that involve the dynamic electron–nucleus coupling have been noted as a pumping process to initiate γ-ray lasers.[15,16] Among them the NEET process has been considered to be a promising mechanism to effectively excite a nucleus to the storage state, which can decay through a radiative transition with the laser characteristics.[15—17] Further studies of NEET are necessary for the application as well as a fundamental study on dynamic interaction between atomic electrons and the nucleus. In addition to NEET induced by the electric-type interaction, it is desirable to obtain the knowledge of NEET induced by the magnetic-type interaction. For muons the magnetic dipole (M1) hyperfine interaction is negligible compared to the E2 interaction.[1,2] In contrast, for electrons the M1 and the E2 interactions are of approximately equal importance, since the former depends upon the magnetic dipole moment which varies inversely with the particle mass. Only in the NEET process, therefore, the nuclear excitation induced by the M1 interaction can be studied and may be observed.

We have tried to detect NEET in ^{197}Au, where NEET is expected to proceed through the M1 interaction. The NEET in ^{197}Au occurs between the excitation of the first nuclear level and the KM electronic transitions, as described later. We have observed the internal conver-

Present address: Department of Chemistry, Faculty of Science, Nagoya University, Chikusa-ku, Nagoya 464-01.
Present address: Faculty of Home Economics, Kobe Women's University, Suma, Kobe 654.
Present address: Department of Information Systems Engineering, Faculty of Engineering, Osaka University, Yamada-Oka, Suita, Osaka 565.
Present address: Department of Electrical and Electronic Engineering, Faculty of Engineering, Osaka Sangyo University, Daito, Osaka 574.

sion electrons emitted from the excited nucleus as an indication of NEET by using a specially designed stroboscopic electron spectrometer. The preliminary experimental results were previously reported.[18] The details of the spectrometer and its performance were also described elsewhere.[19] We describe here the details of the revised data analysis and discuss the NEET process observed in ^{197}Au through a comparison with theoretical predictions that appeared recently.[20—24]

Experimental

Principle of the NEET Observation. Figure 1 shows the NEET diagram for ^{197}Au depicted on the basis of data given in refs 25 and 26. The NEET conditions are satisfied in the KM_1 electronic transition and the 77-keV nuclear excitation, since these transitions have almost equal transition energies and a common multipolarity of M1. The NEET by the E2 interaction may also take place in the $KM_{4,5}$ electronic transitions. The nuclear excitation of the 77-keV level is therefore expected to occur with an appreciable probability following ionization of the K shell of a ^{197}Au atom. As an indication of NEET in ^{197}Au, we selected the internal conversion electrons that are emitted in deexcitation of the first excited nuclear level with a half-life of 1.9 ns.[26]

To observe the conversion electrons, we have developed a stroboscopic electron spectrometer, the principle of which is schematically shown in Fig. 2. The spectrometer consists of two parts, energy analysis and time analysis, and allows us to measure the time spectrum of electrons of a defined energy with a time resolution of subnanoseconds. A ^{197}Au target was bombarded with an electron pulsed beam to ionize the K shell, and the conversion electrons were selected in both energy and time among the secondary electrons emerging from the target.

The electron pulsed beam with an energy of 100 keV, a width of 1 ns, and a repetition of 20 ns, was produced with a pulse gate consisting of high-frequency (25 MHz) deflector I and a chopping aperture. Then secondary electrons emerging from a target bombarded with the electron beam were condensed into a direction perpendicular to the primary beam and deflected again with deflector II working in synchronization with deflector I. The phase difference between the two deflectors was controlled with a phase shifter.[27] The electron beam passing through another aperture after deflection had its momentum analyzed with a magnetic analyzer and finally detected with a Si(Au) detector. The phase difference corresponded to a delay of the emission time of the electrons with a defined energy. We finally detected only the electrons emitted at a delayed time (corrected for the time of flight) corresponding to the phase difference. The phase shifter can delay the phase of deflector II from zero to 50 ns in 0.1 ns increments. A microcomputer system was used to control the phase shifter and to accumulate the data in accordance with the phase difference. Thus, the time spectrum of the electrons with a defined energy can be obtained by scanning the phase difference with the phase shifter as shown in Fig. 2.

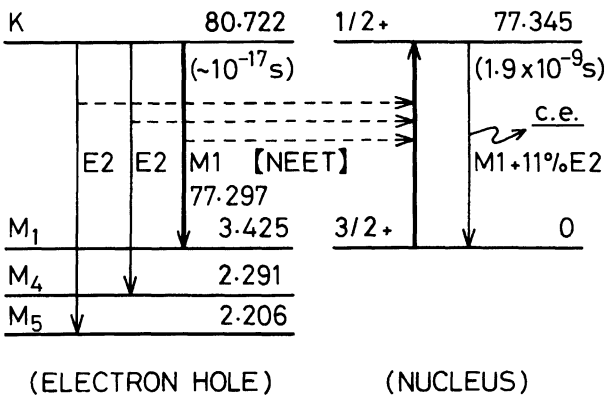

Fig. 1. NEET diagram for ^{197}Au. Energies for each level are given in keV.

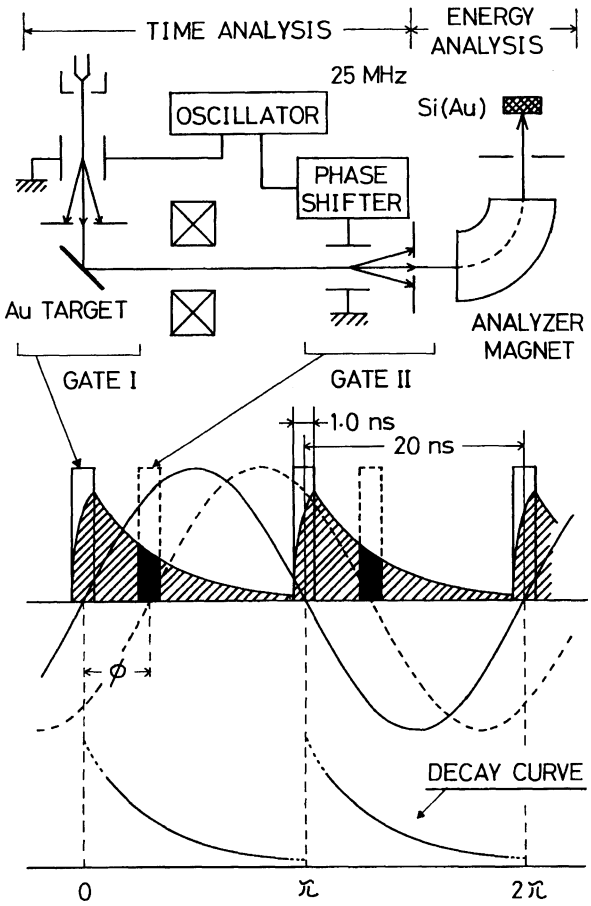

Fig. 2. Principle of the NEET observation system.

In the NEET-observation experiment the analyzer magnet is tuned for the conversion electron of ^{197}Au. If NEET takes place in ^{197}Au, a decay component with a half-life of 1.9 ns is expected to appear on the delayed side of the peak composed of the prompt events in the electron time spectrum. The details of this system are described elsewhere.[19]

Experimental Procedure. A ^{197}Au target was metal foil 10 μm thick and mounted at 45° with respect to both the primary and secondary beam directions. The beam current was typically 60 μA in a DC beam. The analyzer magnet was tuned for 63-keV electrons: This corresponds to the L-conversion electrons, which are a main component of the conversion electrons emitted from the first excited nuclear state. The resolutions of the analyzer magnet and the Si(Au) detector were $\Delta p/p=5\%$ and $\Delta E/E=10\%$, respec-

tively.

A series of measurements consisted of the full region measurement, the valley region one, and again the full region one by which the phase stability was checked. In a typical measurement, scanning was repeated several hundred times with a dwell time per channel of one ms or 40 ms. Figure 3 shows the time spectra of the 63-keV electrons in a single run. The upper (a) and lower (c) spectra for the full region include two peaks (PK-L and PK-R) which are composed of the inelastically scattered electrons and KLM Auger electrons. The energies of the Auger electrons were calculated from data in the literature.[28] The time scale of the obtained spectrum was calibrated using these prompt peaks 20 ns apart. Since the emission of the conversion electrons was delayed compared to the prompt events, only the valley region was further scanned to improve the statistics for the conversion electrons as shown in Fig. 3b. Such a measurement was repeated 60 times. The data were summed up after normalization of the prompt peak positions, and the resultant spectrum, shown in Fig. 4a, was used for the subsequent analysis.

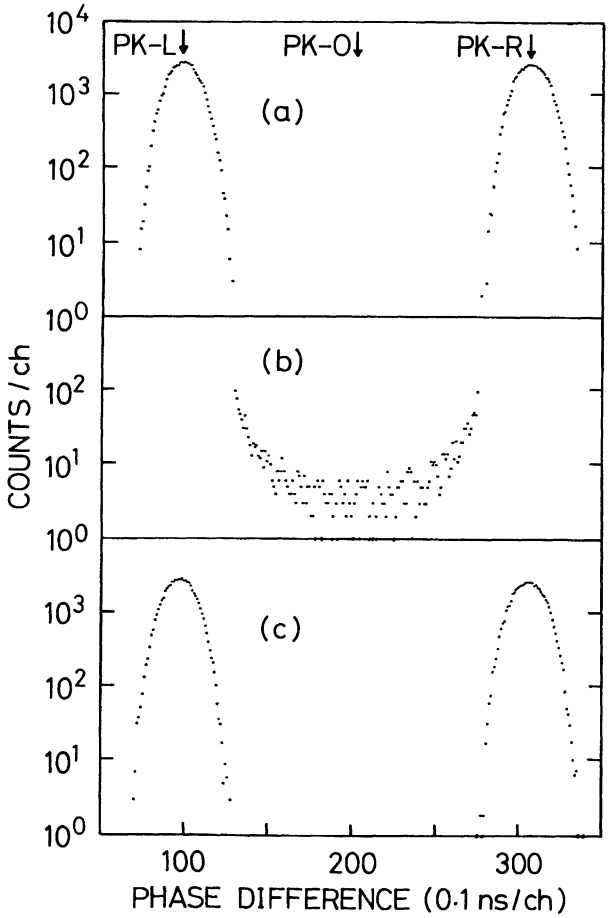

Fig. 3. Typical Time spectrum of 63-keV electrons. (a) Full region (10—40 ns). (b) Valley region. The decay curve due to NEET is expected to appear on the delayed tail. (c) Full region. The instability of the system was checked by comparison to spectrum (a). The abbreviations PK–L and PK–R present the positions of the left and right prompt peak, respectively, and PK–O is the center of the both peaks.

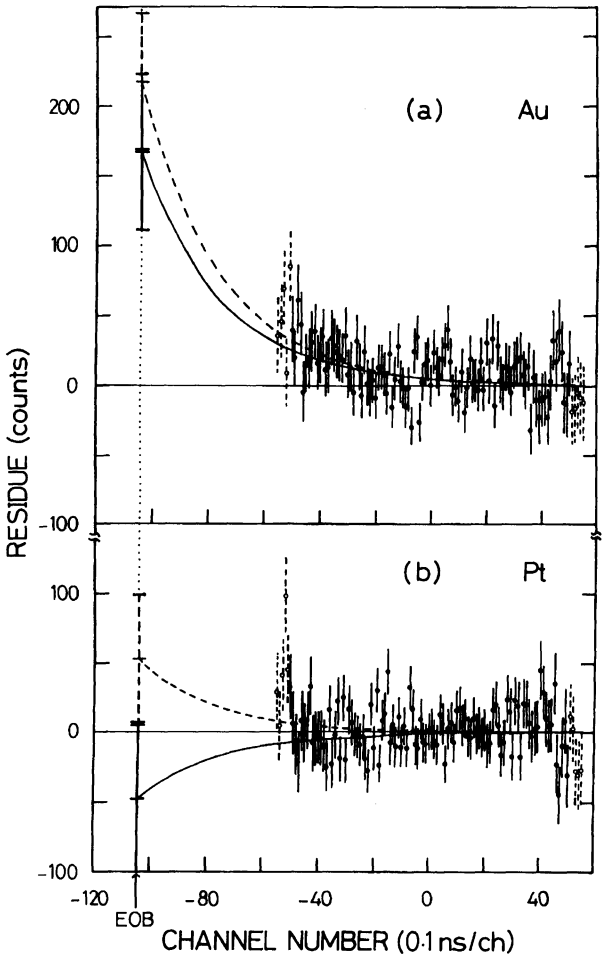

Fig. 4. (a) Residual counts obtained by subtracting the background from the resultant time spectrum of 63-keV electrons for ^{197}Au obtained from the summation of 60 data. (b) Residual counts obtained by subtracting the background from the resultant time spectrum of 63-keV electrons for platinum. The channel number was rearranged about PK–O in the procedure of the data summation. The position of EOB corresponds to the time at the end of bombardment (see text). The solid curve is the decay curve of a half-life of 1.9 ns fitted to them. The fitting region was from 50 to −50 ch (closed circles). The similar results were also obtained in the analysis for another fitting region. Open circles corresponds to the region from 55 to −55 ch and the dashed curve presents the fitting result.

To check the stability of the spectrometer and to measure the background, measurements for platinum (blank experiment) were also done under the same conditions. Platinum is an element neighboring to Au and consists of non-NEET isotopes, accordingly it is the best target for reference. The result for platinum is also presented in Fig. 4b. The details of the measurements were also described elsewhere.[19]

Data Analysis

Decay Function of the Conversion Electrons. The conversion electrons originating from NEET grow

during the irradiation with the electron beam and, when the beam is turned off, they decay with a half-life of 1.9 ns. The growth and decay are repeated with a cycle of 20 ns in this system. According to the literature,[19] the number of the detectable conversion electrons is related to the NEET probability P by the following equation as a function of the phase difference ϕ:

$$C(\phi)=\lambda\varepsilon x n\sigma_K PB\frac{t_s}{T}\frac{4D_0W_0}{\lambda^4\tau_1\tau_2}[1-\exp(-\lambda T)]^{-1}$$
$$[1-\exp(\lambda\tau_1/2)]^2[1-\exp(-\lambda\tau_2/2)]^2\exp[-\lambda(T/2\pi)\phi], \quad (1)$$

for $2\pi\tau_1/T\leq\phi\leq 2\pi(1-\tau_2/T)$, where ϕ is corrected for the flight time of the conversion electron from the target to the gate II. The definitions and values of the parameters used in Eq. 1 are summarized in Table 1. The time dependence in the incident rate of electrons can be approximately expressed in triangular form with the maximum rate D_0 and the irradiation duration τ_1, and the time window of the delayed gate can also be expressed in triangular form with the full window W_0 and the open duration τ_2. The property of the pulsed beam used is described in the literature.[30] Throughout the experiment, τ_1 and τ_2 were set to $\tau_1=\tau_2=2.0$ ns. The value D_0 was also taken as $D_0=6.25\times10^{12}\ I_0$ (μA), where I_0 was the DC (peak) beam current passing through gate I. In addition W_0 was taken as unity. As a consequence, the transmittance in this system was included in the detection efficiency ε. Substitution of these conditions and the tabulated values into Eq. 1 leads to

$$C(\phi)=(3.52\pm0.39)\times10^7\varepsilon P I_0 t_s\exp[-\lambda(T/2\pi)\phi]. \quad (2)$$

Thus, the time variation of the conversion electron shows the normal exponential decay curve with respect to ϕ according to the nuclear decay.

Decay Analysis of the Observed Conversion Electrons. If NEET takes place appreciably, the decay component should appear on the delayed tail of the prompt peak. Both of the time spectra obtained for Au and Pt, however, have similar and smooth shapes, and are apparently symmetric about PK–O. This is conceivable because the decay component caused by NEET is very weak compared with the background level. Then we analyzed both the spectra by using a least squares fitting with a symmetric function about PK–O and extracted the decay component from the asymmetry found for the Au data as described below.

In the extraction of the decay component, it was assumed that the observed spectrum in the valley region was expressed by the following function:

$$Q(\xi)=D(\xi)+B(\xi), \quad (3)$$

where $D(\xi)$ is the decay function:

$$D(\xi)=A_0\exp[-\Lambda\cdot(\xi-\mathrm{EOB})], \quad (4)$$

and $B(\xi)$ is the symmetric background component and represented as an even orders (2n) polynomial:

$$B(\xi)=\sum_{i=0}^{n}k_i\cdot(\xi-\mathrm{RPK\text{-}O})^{2i}. \quad (5)$$

Here, ξ is the relative channel number rearranged in the data summation procedure, the abbreviation EOB means the end of bombardment corresponding to the position of $\phi=0$ and here is taken as the rearranged channel number of PK–L, RPK–O corresponds to PK–O represented by the rearranged channel number, Λ is the decay constant expressed in the units of channel number, A_0 is the count of the decay component at EOB, and k_i is the coefficient of the i-th order in the polynomial.

Using the function $Q(\xi)$, we searched for the best fit to the spectrum obtained, varying the order of the $B(\xi)$ as a parameter, by a least squares method. The best fitted background function was the 8-th orders polynomial. Figure 4 shows the results of analysis for the Au data. The residues obtained by subtraction of the background component $B(\xi)$ indicate that an exponent was left on the delayed tail of the prompt peak, as shown in Fig. 4a. As a result, we obtained $A_0=192\pm58$ counts (reduced chi-squares: $\chi^2_\nu=1.09$) as the number of the conversion electrons detected for the total runs. The selection of data region used for the fitting procedure may affect the value of A_0. Then we analyzed the data for two fitting regions: from -50 ch to 50 ch and from -55 ch to 55 ch, and calculated the A_0 value from two results obtained. The attached error includes the fluctuation due to this effect in addition to the statistical error.

The results of the analysis for the blank experiment are also shown in Fig. 4b. The fitted value of A_0 was obtained as $A_0=1.4\pm57.0$ counts ($\chi^2_\nu=1.16$) for the platinum target, provided that there is an exponential component with a half-life of 1.9 ns. This result evidently indicates that the background is symmetric about PK–O (see Fig. 3) and that there is no exponential residues in the valley region. The exponent found only in the spectrum for ^{197}Au is therefore attributable not to the experimental conditions or accidental causes but to the nuclear decay with a half-life of 1.9 ns.

Next we will consider the uncertainty in A_0 caused by the experimental and analytical procedures, besides the errors described above. The main origins are the fluctuation of time scale due to the instability of the system and the ambiguity of horizontal axis blurred by the data summation process.

The former results in the ambiguity of the symmetric center of the background for each run. This extent is obtained from the error of the prompt peak positions (PK–L and PK–R) and the shift of the peak positions in the first and the last full-region measurements (see Figs. 3a and 3c). This ambiguity, the error of RPK–O, strongly affects the quantity of the exponential component (A_0), because the exponent is much smaller than

Table 1. Parameters Used in Eq. 1 for Derivation of the NEET Probability

Symbol	Description	Numerical value
λ	Decay constant of the 77-keV level in ^{197}Au	3.6×10^{8} s^{-1} a)
x	Thickness of ^{197}Au target (45°)	1.41×10^{-3} cm
n	Atomic density of Au	5.9×10^{22} cm^{-3}
σ_K	Cross section for K-shell ionization in Au	$(4.5\pm0.1)\times10^{-24}$ cm^2 b)
B	Emission probability for conversion electrons	0.809 c)
T	Pulse period	2×10^{-8} s
τ_1	See text	2×10^{-9} s
τ_2	See text	2×10^{-9} s
I_0	Irradiation DC current	60 μA (typically)
t_s	Measuring (sampling) time	1 hour (typically)
ε	Total detection efficiency	1.57×10^{-6} η_T d)

a) Calculated from the half life of 1.9 ns.[26] b) Taken from the literature.[29] c) $B=\alpha/(1+\alpha)$, where $\alpha=4.23\pm0.07$.[26] d) See text.

the background. The average value of the error for 60 data was ±0.36 ch. We evaluated the error of A_0 as ±54%, taking into account both of the above and the statistical error.

The latter comes from the procedure that the data were normalized not to just the position of PK–O but to the nearest channel of PK–O in the summation process. The central channel in the summation was set to an integer of zero. The average value of RPK–O was 0.003 ch, the value of which should approach zero as the number of data is increasing. The shift for the horizontal axis resulting from the summation procedure ranges −0.5 to +0.5 ch naturally. It may be unreasonable that this uncertainty is treated as the standard deviation of statistics. Since this uncertainty, however, was considered to largely affect the exponential component, we deduced the standard deviation of A_0 to evaluated the influence on A_0 by the uncertainty. The standard deviation was obtained with an ordinary method from the difference between the A_0 value for the true RPK–O and the values obtained by the same fitting procedure with the position of RPK–O shifted in the range from −0.5 to +0.5 ch. As a result, the error due to the summation process was estimated as ±34%. Although this treatment is fairly ambiguous, we believe that the uncertainty for the A_0 value due to the system instability and the data analysis is ±62% or less as a whole. The corrected number of the conversion electrons was estimated to be $A_0=191\pm133$ counts.

Estimation of the Total Detection Efficiency. In Eq. 2, the only parameter yet unknown is the detection efficiency of the conversion electrons ε, which is an important factor for measurement of the absolute value of P. The detection efficiency in the system is expressed by

$$\varepsilon = \eta_T\, \varepsilon_C\, \varepsilon_{SCA}\, \varepsilon_D \tag{6}$$

where η_T is a transmission coefficient from the target to the Si(Au) detector of the electrons, ε_C is a detection efficiency of the Si(Au) detector, ε_{SCA} is the fraction of accumulation by the computer system through a single channel analyzer (SCA) relative to the number of signal from the detector, and ε_D is the fraction of the number of the detectable electrons, which emerge from the target surface and enter the detectable solid angle as defined by the aperture placed in the condenser magnet, relative to the total number of the conversion electrons produced in the target. Here we will estimate these values.

η_T is related mainly to the beam alignment and the aperture size. The effect of the latter must be included in η_T because W_0 is set to $W_0=1$. In each run, η_T was obtained from the check of the alignment by DC beam and ranges from 0.6 to 0.9 in the most run. The value of ε_C was calculated as the fraction of the number of the output signal to the number of electrons incident on the detector surface, and estimated to be $\varepsilon_C=0.860$ from the back-scattering coefficient of a 63-keV electron for the surface of the Si(Au) detector.[31] $\varepsilon_{SCA}=0.763$ was also obtained from the window (60.0—66.0 keV) of SCA and the energy spectrum of 63-keV electrons observed by the Si(Au) detector.

Finally ε_D was estimated by the following manner. In Eq. 1, the number of the ionized atoms is calculated by $xn\sigma_K$ per incident electron. But we must indeed take account of the energy degradation, the intensity attenuation, and the scattering of both of the incident and the emitted electrons because of the thick target. Owing to these effects, the spectrum of the conversion electrons emitted from the target surface becomes broad and continuous. Then, we estimated the energy spectrum of the conversion electrons emitted within the solid angle subtended by an aperture placed in the condenser magnet by the Monte Carlo method as follows and determined the ε_D value.

For low energy electrons running in the solid phase, a collision with a nucleus changes the direction of the motion and that with an orbital electron degrades the energy. According to Lindhard et al.,[32] the energy loss and the differential cross section for the nuclear collision are expressed by

$$\frac{dE}{dx} = -\pi\lambda_s \frac{2^{2/s-1} a^{2-2/s} e^{4/s} n Z}{1-1/s} E^{1-1/s}, \quad (7)$$

and

$$\frac{d\sigma_n}{d\theta} = \pi\lambda_s \frac{2^{1/s-1} a^{2-2/s} e^{4/s} Z^{2/s}}{E^{2/s}} \cdot \frac{\sin\theta}{(1-\cos\theta)^{1+1/s}}, \quad (8)$$

respectively, where λ_s and s are the empirical constants, Z is the target atomic charge, n is the atomic density, e is the electron charge, and $a=0.8853 \cdot a_H Z^{-1/3}$, with a_H being the Bohr radius. We used the values $\lambda_s=0.182$ and $s=6/5$ which are in good agreement with the experiments in the range from 10 to 1000 keV.[33]

In the calculation, the scattering event of the electron was generated based on the mean free path given by $1/(n\sigma_n)$. The energy loss was estimated from the dE/dx and the path length, and the scattering angle was determined randomly with the weight of $d\sigma_n/d\theta$. Doing the Monte Carlo simulation consisting of the above processes, we obtained the distribution of the ionized atoms along the depth coordinate and the trajectories of the conversion electrons. The latter gives all path lengths from the initial position, where the ionized atom emits a conversion electron as a consequence of NEET, to the target surface. As a result, we obtained the energy spectrum of the conversion electron emitted from the target surface. The calculation was done for all related conversion lines, the intensities and energies of which were estimated from the conversion coefficients and the energies of electronic levels in the literature,[34] taking M1+11%E2 as the nuclear transition type. The obtained spectrum of the L_1-conversion electron is shown in Fig. 5 as an example.

The number of the conversion electrons passing through the momentum window of the analyzer magnet was estimated to be $N=7.28\times10^{-10}$ per primary incident electron from the spectra predicted for all lines.

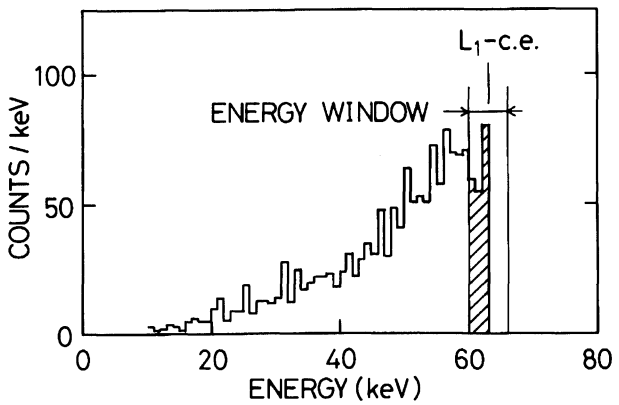

Fig. 5. Spectrum obtained by the Monte Carlo simulation for the L_1-conversion electron. 10000 events were generated in the calculation. The shaded region shows the conversion electrons passing through the energy window of the analyzer magnet. The similar spectra were also obtained for the L_2-, L_3-, M_1-, ···, N-conversion electron.

Thus ε_D was estimated to be $\varepsilon_D=2.4\times10^{-6}$ from the ratio of N to $xn\sigma_K B$. Consequently, we obtained $\varepsilon=1.57\times10^{-6}\ \eta_T$ as the total detection efficiency.

Derivation of the NEET Probability. Although the observed decay component had a large uncertainty in the value, it may be concluded that the nuclear excitation via the NEET process was detected in ^{197}Au because no phenomenon except NEET could explain the asymmetric component appearing only in the case of ^{197}Au as described above. Since the obtained A_0 value is the sum count of 60 times runs, it can be related to the NEET probability P by the following:

$$A_0 = \sum_{i=1}^{60} C_i(\phi=0) = (55.2\pm6.2)\cdot P \sum_{i=1}^{60} \eta_{T_i} I_{0_i} t_{s_i}, \quad (9)$$

using Eq. 2 and the value of ε, where C_i means the number of the conversion electrons detected in the i-th run, and η_{T_i}, I_{0_i}, and t_{s_i} are the transmission coefficient of the conversion electrons, the DC electron beam current, and the sampling time, respectively, for the i-th run. The summation part of Eq. 10 corresponding to the total current was

$$\sum_{i=1}^{60} \eta_{T_i} I_{0_i} t_{s_i} = 68529\ (\mu C). \quad (10)$$

Consequently, the NEET probability was deduced to be $P=(5.1\pm3.6)\times10^{-5}$.

This value is smaller by a factor of four than the previous one.[18] The discrepancy comes mainly from the different treatments for the beam pulse width in data analysis and for the detection efficiency ε_D. In our previous report, we set simply $\tau_1=\tau_2=1$ ns from the deflection frequency and the aperture width. In expressing the pulse shape with a triangular form, however, it is more reasonable to take $\tau_1=\tau_2=2$ ns as the present case is, since the result of measurement for the ratio of pulsed to DC beam current shows the average pulse width to be 1 ns.[19] We also evaluated the ε_D with an elaborate method and obtained the more probable value of ε_D in this report. Therefore, this value is considered to be more reliable, in spite of large discrepancy between the present and the previous one.

Discussion

We must consider the other mechanism to activate the nucleus of ^{197}Au, before discussion of the observed NEET process. Another possible mechanism for the nuclear excitation is Coulomb excitation by inelastically scattered electrons. The cross section for ^{197}Au with 100-keV electrons was calculated according to the theoretical treatment by Alder et al.[35] with $B(M1)=7.75\times10^{-3}\ \mu_N^2$ and $B(E2)=0.13\ e^2b^2$.[26] The applicability to the energy region well below 1 MeV has been experimentally confirmed by Saito et al.[36] The estimated cross section was 9.3×10^{-9} b, while the observed one responsible for the nuclear excitation was 8.1×10^{-4} b. Then it was concluded that the contribution of the

Table 2. Comparison among the Theoretical and Observed NEET Probabilities

Nuclide	Experimental	(Interaction)	Theoretical				
			Pisk et al.[a]	Morita et al.[b]	Ho et al.[c]	Ljubičić et al.[d]	Tkalya[e]
^{189}Os	$(1.7\pm0.2)\times10^{-7}$ [f]	(E2+M1)	2.5×10^{-7}	5.9×10^{-11}	1.2×10^{-9}	2.3×10^{-7}	3.4×10^{-10}
	4.3×10^{-8} [g]						
	$(1.2\pm0.8)\times10^{-8}$ [h]						
	$(5.7\pm1.7)\times10^{-9}$ [i]						
^{197}Au	$(5.1\pm3.6)\times10^{-5}$ [j]	(M1)	3.5×10^{-5}		4.2×10^{-7}	2.2×10^{-5}	1.3×10^{-7}
^{237}Np	$(2.1\pm0.6)\times10^{-4}$ [k]	(E1)	1.5×10^{-7}		8.5×10^{-9}	2.6×10^{-4}	3.1×10^{-12}

a) Ref. 20. b) Ref. 21. c) Ref. 22. d) Ref. 23. e) Ref. 24. f) Ref. 10. g) Ref. 11. h) Ref. 12. i) Ref. 13. j) Present work. k) Ref. 14.

Coulomb excitation process was negligible and hence the observed activity of ^{197}Au was attributed to only the NEET process.

Here, we will discuss the NEET process in ^{197}Au from comparisons with several theoretical predictions. The NEET probability P can be estimated theoretically by

$$P = (1+\Gamma_2/\Gamma_1)E'^2/\{\Delta^2+[(\Gamma_1+\Gamma_2)/2]^2\}, \quad (11)$$

according to the literature,[9,10] where Γ_1 and Γ_2 are the level widths of the initial and final electronic states participating in NEET, respectively, E' is the electromagnetic interaction energy between the nucleus and its orbital electrons, and Δ is the energy difference between the electronic and the nuclear transitions. In ^{197}Au, $\Delta=-48$ eV,[25,26] $\Gamma_K=49.6$ eV,[37] and $\Gamma_{M1}=20.9$ eV,[38] since the NEET conditions are satisfied in the KM_1 electronic transition and the 77-keV nuclear transition as shown in Fig. 1.

The amount of E' for the M1 interaction can be very roughly estimated from the Bohr and nuclear magnetons (μ_B and μ_N) and the electron density at the nucleus by the following formula:[39]

$$E' = -\frac{8\pi}{3}\,\mu_B\left(\frac{g_p}{2}\right)\mu_N\,\psi_{1s}(0)\,\psi_{ns}(0), \quad (12)$$

where g_p is the gyromagnetic factor of proton and $\psi_{1s}(0)$ and $\psi_{ns}(0)$ are the 1s- and ns-electron wave functions at the nucleus. By using the results of calculation with the relativistic Dirac–Fock equations[40] as the values of the wave functions, we obtained $P=2.3\times10^{-4}$, which was larger by a factor of four than the observed one. However, if considering for the dynamic reduced matrix element B(M1) of the relevant transition to be smaller than the magnetic moment of proton, the estimate for M1 may be also smaller by one or two orders of magnitude than the crude estimate described above which is dealt with a kind of a single particle estimate.

The more detailed calculations for P have been recently developed by many authors.[20—24] Morita et al.[21] and Ho et al.[22] formulated the interaction E' by means of a time dependent perturbed method and Ho et al. obtained $P=4.2\times10^{-7}$ for ^{197}Au by using the published data for B(M1) and Γ_i. Tkalya[24] discussed the NEET probability in the framework of quantum electrodynamics (QED) and obtained $P=1.3\times10^{-7}$ for ^{197}Au. These were smaller by two orders of magnitude than the experimental value.

Different approaches to the estimation for P have been also proposed by Pisk et al.[20] and Ljubičić et al.[23] The formalism by Pisk et al. expressed the P value in terms of the excited nuclear level width, the energy difference between the nuclear and electron transitions, the Coulomb interaction between the initial electron states, and the electron level width. Ljubičić et al. dealt with the NEET phenomenon by a similar treatment as Pisk et al, but declared that the probability depends on the atomic parameters only. Both of them obtained the P values in reasonable agreement with the experimental results for other NEET-nuclides as well as ^{197}Au.

A comparison among these theoretical estimates is shown in Table 2 for all NEET-nuclides observed. One can see that the theoretical treatment for NEET is still controversial, although the approaches by Pisk et al. and Ljubičić et al. better explain the experimental results. The status of the recent theoretical treatments has been reviewed by Tkalya.[41]

In addition to the M1 interaction, the NEET by the E2 interaction in ^{197}Au may occur between the $KM_{4,5}$ electronic transitions and the 77-keV nuclear transition as shown in Fig. 1. We then evaluated the contribution of NEET induced by the E2 interaction by a crude estimate, since the theoretical predictions for ^{197}Au have not been reported so far. A simple formula for E' employed in the original NEET theory[9,10] provides $P=3\times10^{-5}$, taking account of the enhancement of the nuclear matrix element by the collective motion. This means that the E2 component may be not negligible for NEET in ^{197}Au, although the relevant nuclear transition has a small E2 fraction. Anyway, more reliable theoretical consideration is required for the NEET by E2 interaction as well as M1 interaction to discuss the mechanism of the NEET process in ^{197}Au.

Conclusion

The decay component of a half-life of 1.9 ns was observed in the 63-keV electron time spectrum taken with a nanosecond stroboscopic electron spectrometer by bombarding ^{197}Au with 100-keV pulsed electron

beam. The observed activity was ascribed to the decay of the 77-keV nuclear level having been excited by the NEET process. We concluded that the NEET phenomenon was observed in ^{197}Au and the probability was $P=(5.1\pm3.6)\times10^{-5}$, taking account of the reliability for the experimental method checked by the blank measurements and for the elaborate method of the data analysis, although the obtained value had a large uncertainty. The revised NEET probability for ^{197}Au reported here will be useful for the progress of the NEET theory as the third example following ^{189}Os[10—13] and ^{237}Np.[14]

We gratefully acknowledge the valuable assistance of Mr. T. Kadota and Mr. S. Morimoto in the various phase of this experiment. We are greatly indebted to Dr. M. Morita for his helpful discussion on the theoretical treatment. We also express our gratitude to Dr. R. Arakawa, Dr. K. Nakamae, Dr. H. Baba, and Dr. M. Furukawa for their interests and encouragements.

References

1) L. Wilets, *Dan. Mat. Fys. Medd.*, **29**, 3 (1954).
2) B. A. Jacobsohn, *Phys. Rev.*, **96**, 1637 (1954).
3) J. Z. Hüfner, *Z. Phys.*, **190**, 81 (1966).
4) S. Bernow, S. Devons, I. Duerdoth, D. Hitlin, J. W. Kast, W. Y. Lee, E. R. Macagno, J. Rainwater, and C. S. Wu, *Phys. Rev. Lett.*, **21**, 457 (1968).
5) Y. Yamazaki, E. B. Shera, M. V. Hoehn, and R. M. Steffen, *Phys. Rev. C*, **18**, 1474 (1978).
6) W. W. Wilcken, M. W. Johnson, W. U. Schröder, J. R. Huizenga, and D. G. Perry, *Phys. Rev. C*, **18**, 1452 (1978).
7) W. U. Schröder, W. W. Wilcke, M. W. Johnson, D. Hilscher, J. R. Huizenga, J. C. Browne, and D. G. Perry, *Phys. Rev. Lett.*, **43**, 672 (1979).
8) J. N. Bradbury, M. Leon, H. Daniel, and J. J. Reidy, *Phys. Rev. Lett.*, **34**, 303 (1975).
9) M. Morita, *Prog. Theor. Phys.*, **49**, 1574 (1973).
10) K. Otozai, R. Arakawa, and M. Morita, *Prog. Theor. Phys.*, **50**, 1771 (1973); K. Otozai, R. Arakawa, and T. Saito, *Nucl. Phys. A*, **A297**, 97 (1978).
11) T. Saito, A. Shinohara, T. Miura, and K. Otozai, *J. Inorg. Nucl. Chem.*, **43**, 1963 (1981).
12) L. Lakosi, I. Pavlicsek, Z. Németh, and Á. Veres, "Proc. Int. Symp. on Symmetries and Nuclear Structure, Dubrovnik (1986)," ed by R. A. Meyer and V. Paar, Harwood Academic, Chur (1986), p. 568.
13) A. Shinohara, T. Saito, M. Shoji, A. Yokoyama, H. Baba, M. Ando, and K. Taniguchi, *Nucl. Phys. A*, **A472**, 151 (1987).
14) T. Saito, A. Shinohara, and K. Otozai, *Phys. Lett. B*, **92B**, 293 (1980).
15) G. C. Baldwin, J. C. Solem, and V. I. Goldanskii, *Rev. Mod. Phys.*, **53**, 687 (1981).
16) D. W. Noid, F. X. Hartmann, and M. L. Koszykowski, "AIP Conf. Proc., No. 160," 69 (1987); G. A. Rinker, J. C. Solem, and L. C. Biedenharn, "AIP Conf. Proc., No. 160," 75 (1987); J. A. Bounds, P. Dyer, and R. C. Haight, "AIP Conf. Proc., No. 160," 87 (1987).
17) K. Okamoto, *Nucl. Phys. A*, **A341**, 75 (1980).
18) H. Fujioka, K. Ura, A. Shinohara, T. Saito, and K. Otozai, *Z. Phys. A*, **A315**, 121 (1984).
19) H. Fujioka and K. Ura, *J. Appl. Phys., Jpn.*, **24** 1703 (1985).
20) K. Pisk, Z. Kaliman, and B. A. Logan, *Nucl. Phys. A*, **A504**, 103 (1989).
21) M. Morita, H. Ohtsubo, T. Sato, and K. Oka, "Governmental Report for Grand-in-Aid for Scientific Research of Japan," (in japanese), Tokyo (1990).
22) Y. K. Ho, B. H. Zhang, and Z. S. Yuan, *Phys. Rev. C*, **44**, 1910 (1991).
23) A. Ljubičić, D. Kekez, and B. A. Logan, *Phys. Lett. B*, **272B**, 1 (1991).
24) E. V. Tkalya, *Nucl. Phys. A*, **A539**, 209 (1992); E. V. Tkalya, *JETP Lett.*, **56**, 131 (1992).
25) "Table of Isotopes," 7th ed, ed by C. M. Lederder and V. S. Shirley, Wiley, New York (1978).
26) B. Harmatz, *Nucl. Data Sheets*, **34**, 101 (1981).
27) H. Fujioka, K. Nakamae, and K. Ura, *J. Phys. E*, **17**, 198 (1984).
28) F. P. Larkins, *At. Data Nucl. Data Tables*, **20**, 331 (1977).
29) D. V. Davis, V. D. Mistry, and C. A. Quarles, *Phys. Lett. A*, **38A**, 169 (1972).
30) H. Fujioka and K. Ura, *Scanning*, **5**, 3 (1983).
31) T. Tabata, R. Ito, and S. Okabe, *Nucl. Instrm. Methods*, **94**, 509 (1971).
32) J. Lindhard, M. Scharff, and H. E. Schiøtt, *Dan. Mat. Fys. Medd.*, **33**, 1 (1963).
33) K. Kanaya and S. Okayama, *J. Phys. D*, **5**, 43 (1972).
34) F. Rosel, H. M. Fries, K. Alder, and H. C. Pauli, *At. Data Nucl. Data Tables*, **21**, 291 (1978).
35) K. Alder, A. Bohr, T. Huus, B. Mottelson, and A. Winther, *Rev. Mod. Phys.*, **28**, 432 (1956).
36) T. Saito, Y. Ohkubo, A. Shinohara, R. Arakawa, and K. Otozai, *Nucl. Phys. A*, **A330**, 443 (1979).
37) H. J. Leisi, J. H. Brunner, C. F. Perdrisat, and P. Scherrer, *Helv. Phys. Acta*, **34**, 161 (1961).
38) E. J. McGuire, *Phys. Rev. A*, **5**, 1043 (1972).
39) M. Morita, private communication (1979).
40) I. M. Band and V. I. Fomichev, *At. Data Nucl. Data Tables*, **23**, 295 (1979).
41) E. V. Tkalya, *Sov. Phys. JETP (Engl. Transl.)*, **75**, 200 (1992).